

Donor level of bond-center hydrogen in germanium

L. Dobaczewski*

Institute of Physics, Polish Academy of Sciences, al. Lotników 32/46, 02-668 Warsaw, Poland

K. Bonde Nielsen, N. Zangenberg, and B. Bech Nielsen

Institute of Physics and Astronomy, University of Aarhus, Ny Munkegade, DK-8000 Århus C, Denmark

A. R. Peaker and V. P. Markevich

Centre for Electronic Materials, University of Manchester Institute of Science and Technology, P. O. Box 88, Manchester M60 1QD, United Kingdom

(Received 17 December 2003; published 28 June 2004; corrected 11 August 2004)

We apply Laplace deep-level transient spectroscopy (LDLTS) *in situ* after low-temperature proton implantation into crystalline *n*-type germanium and identify a deep metastable donor center. The activation energy of the donor emission is ~ 110 meV when extrapolated to zero electric field. We obtain the split patterns of the emission signal for uniaxial stress applied along three major crystal directions $\langle 100 \rangle$, $\langle 110 \rangle$, and $\langle 111 \rangle$, and conclude that the symmetry of the center is trigonal. We compare the annealing characteristics with those of bond-center hydrogen in silicon and with those of a trigonal center in germanium previously identified as bond-center hydrogen by *in situ* local-mode infrared absorption spectroscopy. From this comparison it is concluded that the observed donor emission originates from bond-center hydrogen. Infrared absorption also revealed another trigonal center tentatively ascribed to hydrogen occupying an antibonding configuration. A search for a corresponding deep level (as a hole or electron trap) failed, indicating that such level must be near midgap or resonant with (close to) the valence band.

DOI: 10.1103/PhysRevB.69.245207

PACS number(s): 61.72.Cc, 61.72.Tt, 71.55.Cn

I. INTRODUCTION

The isolated hydrogen impurity in silicon has been studied extensively in the past theoretically as well as experimentally.^{1,2} See also the review by Estreicher³ and the recent articles, Refs. 4–6. The impurity may exist in three different charge states H^+ , H^0 , and H^- depending on which site in the silicon lattice hydrogen occupies. These charge states give rise to either a donor level ($0/+$) ascribed to hydrogen at the bond-center site (BC) or an acceptor level ($-/0$) defined as the change in energy when hydrogen emits an electron and as a result swings from the tetrahedral site (T) to the BC site. An important feature, predicted theoretically^{7,8} and confirmed experimentally,⁶ is the inverted order of the donor and acceptor levels (i.e., the negative- U property). In other words either H_{BC}^+ or H_T^- is the stable configuration for any position of the Fermi level and the neutral charge state H_{BC}^0 is always metastable (and has slightly lower total energy than H_T^0). Hence, when the hydrogen impurity is thermodynamically able to capture an electron, then the lowest energy configuration is H_T^- . When the electron capture process is not possible, then this configuration is H_{BC}^+ . According to theory,⁷ which has been supported experimentally in several ways, the crossing point for formation energies of H_T^- and H_{BC}^+ corresponds to the Fermi-level position slightly above midgap. Therefore, disregarding the possibility of having metastable configurations at low temperature, the hydrogen atom will act as an amphoteric impurity, i.e., tending to attain a positive charge state in *p*-type material and (as long as the *n*-type resistivity is not too high) a negative charge state in *n*-type material. A simple consequence of this is that in pure silicon the diffusion barrier of interstitial hydrogen⁹

is close to the barrier measured for hydrogen jumping between bond-center sites.^{10,11} This picture may break down at low temperature for two reasons. (i) The trapping at impurities or intrinsic defects tends to slow down, and eventually stop, the migration of hydrogen by forming stable centers. (ii) The metastable configurations of hydrogen may speed up its migration predominately due to the presence of fast migrating H_T^0 , which is assumed to be generated transiently in *n*-type material over a narrow temperature range where the actual Fermi level matches the H_{BC}^+/H_T^- crossing point. In addition to the available data for hydrogen^{4–6} some of the essential activation processes governing the hydrogen dynamics in silicon have been revealed also by muon-spin techniques.^{12,13} Allowing for isotopic differences in zero-point energies the agreement between the hydrogen and muon data is satisfactory. Both types of studies accentuate the significance of the hydrogen charge state in the migration process.

In germanium one may expect to find similar defect configurations.³ It has been shown theoretically¹⁴ that also in this case a negative- U behavior of the isolated hydrogen centers can be expected. However the details of the dynamics, which depends critically on the level position and saddle point energies, may be quite different. The explicit calculations¹⁴ and recent systematics¹⁵ indicate that the ($-/0$) level of hydrogen at the tetrahedral interstitial site should be resonant with the valence band. This is in contrast to the case of silicon, where this level is midgap, below the donor level, with the amphoteric behavior as one of the consequences. The only direct experimental information on isolated hydrogen in germanium obtained so far comes from a recent infrared absorption study¹⁶ in which *in situ* spectroscopy after low-temperature implantations revealed a strong

stretch-mode signal, which in all its properties resembles that of the established stretch-mode absorption of bond-center hydrogen in silicon. This signal was consequently ascribed to the germanium analog of this center. In addition a weaker (but still strong) mode was ascribed to the degenerate bend mode of hydrogen in an antibonding configuration (AB).

The present article describes a search for the donor and acceptor levels of isolated interstitial hydrogen in germanium through *in situ* application of high-resolution deep-level transient spectroscopy (Laplace DLTS) carried out in a way analogous to the *in situ* infrared absorption work.¹⁶ As in the case of silicon it is essential to know the positions of the donor and acceptor levels in order to understand hydrogen doping and hydrogen dynamics in germanium. Neither of the two levels has been identified so far, although muonium results¹⁷ indicate the existence of bond-center donor emission with an activation energy of ~ 0.23 eV. In addition, shallow acceptor-type centers have been ascribed to hydrogen trapped at substitution-site C or Si impurities.¹⁸ These centers are trigonal¹⁹ antibonding-type defects, which may form when the migrating hydrogen enters a tetrahedral interstitial site next to the impurity. From theory their $(-)/0$ levels are expected to be similar to the corresponding level of isolated hydrogen.

II. TECHNICAL DETAILS

A. Sample preparation

For the application of the DLTS technique Schottky diodes were prepared on samples cut and polished from Czochralski-grown antimony-doped bulk germanium. Two sets of sample materials with Sb concentrations of $\sim 1.5 \times 10^{15} \text{ cm}^{-3}$ and $\sim 3 \times 10^{14} \text{ cm}^{-3}$ were used. The sample materials were obtained from two different suppliers (Union Miniere, Belgium, and Belarussian State University, Minsk, respectively). In both materials the concentration of interstitial oxygen was determined by infrared absorption to $\sim 7 \times 10^{16} \text{ cm}^{-3}$. For the uniaxial stress measurements sample bars of $1 \times 2 \times 7$ mm were cut from the Minsk material and polished in a $\langle 110 \rangle$ plane with edges cut along $\langle 100 \rangle$, $\langle 110 \rangle$, or $\langle 111 \rangle$ directions, respectively. All samples were furnished with Schottky diodes made by thermal evaporation of 1.3 mm^2 gold dots.

B. Experimental procedure

The samples (two at a time) were mounted on the cold finger of a cryocooler and implanted with protons (or helium ions for control measurements) at a temperature of 50 K. The implantation energy was chosen for the individual samples so that the peak of the implants would match the depletion width of the diode under suitable reverse bias. For hydrogen implantation of the Belgian material this energy was typically 600 keV, corresponding to a reverse bias of ~ 3.5 V. In this way we could perform subsequent *in situ* DLTS measurements utilizing the Laplace method²⁰ to deconvolute composite capacitance transients into emission-rate spectra. The sample bias was normally chosen to place the implantation profile close to the edge of the reverse-bias depletion

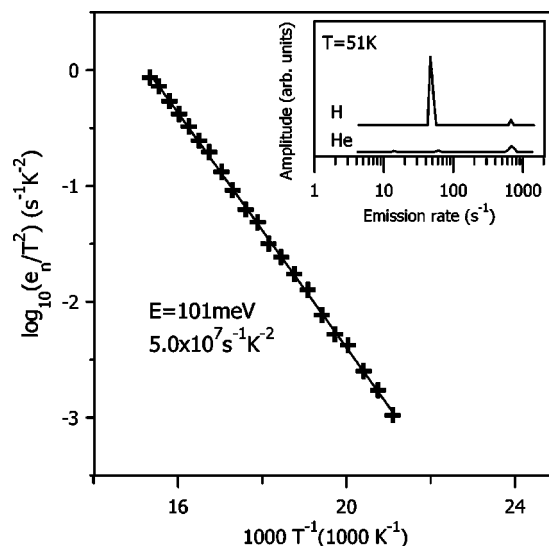


FIG. 1. *In situ* Arrhenius analysis of the dominant Laplace DLTS signal recorded at low temperature after proton implantation at 50 K into a short-circuited Au Schottky diode. The signal originates from the proton stopping range. It is hydrogen related as the inset shows by comparison of equivalent H and He implantations.

layer in order to minimize the electric field at the depth of the implants and at the same time to maximize the amplitude of the DLTS signals. The implantations were monitored *in situ* by CV profiling. Samples with $\leq 20\%$ compensation at the peak of the implants could be utilized maintaining an exponential shape of the individual capacitance transients.

Besides the improved resolution, a special feature of the Laplace method is that isothermal emission-rate spectra are recorded, which makes the method particularly suitable for annealing and uniaxial-stress studies. In the present study we first examined the “as-implanted samples” in the temperature range from the implantation temperature of 50 K up to 100 K. Then isochronal annealing sequences were carried out with and without bias on the sample diodes and emission spectra were recorded at suitable temperatures in the range 50–100 K for different choices of rate windows. At lower temperatures and with open-face samples the thermal radiation impinging from the walls of the implantation chamber typically causes emission peaks to shift towards higher rates.²¹ These optically induced shifts were also observed in the present case but were eliminated by covering the beam entrance of the cooled sample holder during data recording.

III. RESULTS AND ANALYSIS

A. Identification of hydrogen-related donor emission

The inset of Fig. 1 depicts the Laplace DLTS spectra obtained at 51 K after implanting hydrogen at 50 K into short-circuited Au Schottky diodes at a dose of $\sim 6 \times 10^8 \text{ cm}^{-2}$. Prior to the implantation no signal is present in the displayed emission-rate range and only very small and insignificant process-induced signals were revealed (by conventional DLTS) during cooling of the sample from room temperature. The spectrum for the proton implanted sample is compared

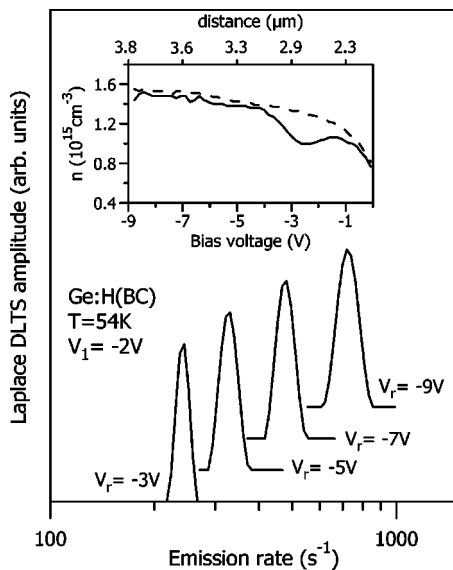


FIG. 2. Electric field dependence of emission rates demonstrating its donor character where the shift in rate as a function of bias voltage is shown. The inset shows the carrier concentration derived from the *CV* profile before and after implantation as dashed and solid lines, respectively. The dip in the carrier profile at around -2.8 V coincides with the peak concentration of the hydrogen implant. The upper scale of the inset marks the depths corresponding to the biases given by the lower scale (note: the upper scale is nonlinear).

to a spectrum obtained after implantation of helium at a dose of $\sim 2 \times 10^8 \text{ cm}^{-2}$ into an identical diode. No significant majority-carrier emission other than the peak shown appears in the range 0.05 to $5 \times 10^3 \text{ s}^{-1}$ examined at suitable temperatures below 100 K. In addition we observed small minority-carrier signals at low temperature caused by injection of holes from the Schottky junction. We cannot exclude that these signals (in part) could be associated with hydrogen. However, because most of the signals are present prior to the implantation they may have been introduced during the HF rinse applied in the diode fabrication and are therefore not introduced as a result of the implantation. We shall return to this point in further detail in Sec. III C.

The comparison in Fig. 1 of the hydrogen and helium data show unambiguously that the recorded emission peak is related to hydrogen, in perfect analogy with previous results⁴ for the dominant center formed during low-temperature hydrogen implantation into silicon. For a quantitative (dose independent) comparison of the production yield of the dominant hydrogen centers in Ge and Si we further carried out a simultaneous *in situ* implantation of closely positioned Schottky diodes build on Ge and Si substrates. From these measurements we conclude that the yield at 50 K is larger by a factor of ~ 1.9 for Si than for Ge with the peak intensity accounting for $\sim 30\%$ of the implanted hydrogen in the case of Ge. Possible reasons for this difference are discussed later. However, the relatively large fractions of implants accounted for clearly demonstrate the similarity of the two cases. As for Si the dominating electron emission in Ge most likely originates from a center of interstitial type with hydrogen squeezed into the germanium host lattice as a direct result of

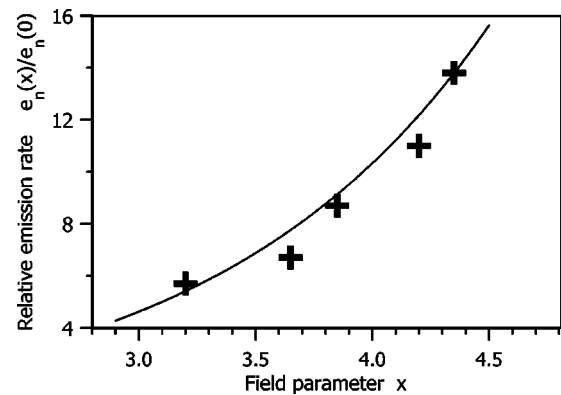


FIG. 3. Field dependence compared to the three-dimensional Hartke model (Ref. 23) as explained in the text. The field parameter x is given by $(e^3 F / \pi \epsilon)^{1/2} / k_B T$, where F is the magnitude of the electric field, e the elementary charge, and ϵ the dielectric constant of Ge.

the implantation process. In Fig. 1 we also depict an Arrhenius analysis of the peak position, yielding an activation enthalpy of $\Delta H = 101 \pm 2$ meV. The relatively large value of the preexponential factor indicates that we are dealing with a donor signal.

In order to confirm the donor character of the defect we examined the electric field dependence of the signal as indicated by the data shown in Figs. 2 and 3. The implantation depth on the voltage scale is around -3 V as confirmed by the voltage dependence of the peak intensities and *CV* profiling (see inset in Fig. 2). Note that the hydrogen donor signal is observed on the shallow donor compensation profile slightly shifted towards the left shoulder partly as a result of the donor artifact²² and partly because the compensation peak due to implantation damage is shifted slightly towards the junction as compared to the true hydrogen depth. At this depth we estimate the electric field as a function of reverse bias and conclude that the observed field dependence of the emission rate within an uncertainty of about 25% is in agreement with the prediction of the Hartke model²³ for a single donor (see Fig. 3). On this basis the zero field value of the activation enthalpy may be estimated as $\Delta H = 110 \pm 4$ meV.

In the case of bond-center hydrogen in silicon the zero field activation enthalpy has been determined to be 175 ± 5 meV.⁴ As briefly outlined in the Introduction we can expect that hydrogen behaves similarly in germanium and silicon. For silicon it has been established⁴ by equivalent *in situ* measurements that a large fraction (typically $\sim 60\%$) of the hydrogen implants enters the metastable bond-center configuration revealed by its donor emission. Hence, the similarity of the two cases suggests that also for germanium a neutral metastable BC configuration of hydrogen forms during implantation with most of the remaining implants hidden as negatively charged hydrogen at or near T sites. With the Si/Ge analogy in mind we anticipate our final assignment of the donor signal and denote it EH_{BC} . This bond-center assignment is substantiated by uniaxial-stress and annealing measurements to be presented in the next section.

B. Symmetry and annealing

A defect structure with monatomic hydrogen atoms located in a $\langle 111 \rangle$ directed Ge-Ge bond of crystalline Ge must

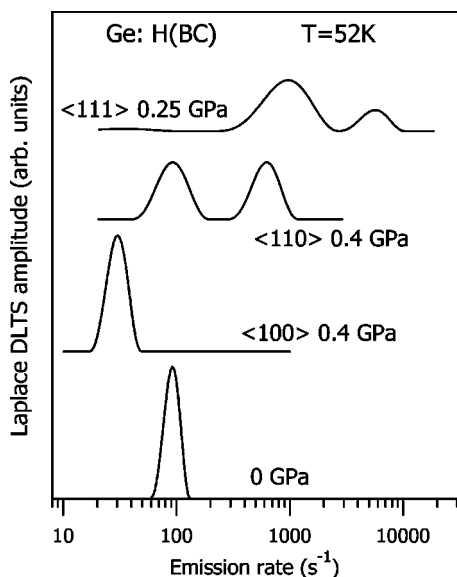


FIG. 4. Uniaxial-stress split patterns of the donor emission signal (see Fig. 1). The intensity ratios are 3:1 for stress along $\langle 111 \rangle$, 2:2 for stress along $\langle 110 \rangle$, and 4:0 for stress along $\langle 100 \rangle$, revealing the trigonal symmetry of the emitting center.

exhibit trigonal symmetry. In order to determine the symmetry of the EH_{BC} center we carried out a series of uniaxial-stress measurements applying the stress along the three major crystallographic directions. The results are depicted in Fig. 4. As can be seen the application of stress along $\langle 111 \rangle$ and $\langle 110 \rangle$ causes 3:1 and 3:2 splitting, respectively, whereas $\langle 100 \rangle$ stress does not cause any splitting. The splitting patterns confirm the trigonal symmetry of the emitting center, and thereby support the anticipated ascription of this signal to bond-center hydrogen.

As stated in the Introduction, *in situ* local-mode spectroscopy applied to low-temperature hydrogen implanted intrinsic germanium has revealed a dominant infrared active center also of trigonal symmetry. This center anneals at ~ 225 K, and if it is identical to our designated EH_{BC} center, the annealing properties of the two centers should be similar. We show this in Fig. 5. Here, the filled circles mark isochronal annealing sequences carried out for EH_{BC} in 10 min steps with reverse bias applied during the annealing. For comparison we include the data (open symbols) taken from Budde *et al.*¹⁶ These data represent the result of isochronal annealing (in 15 min steps) of the 1794 cm^{-1} infrared absorption line. This line has been identified unambiguously as the stretch mode absorption of bond-center hydrogen in the positive charge state and its annealing properties should therefore be compared to those of the EH_{BC} defect in its ionized state. As can be seen the reverse-bias annealing of the EH_{BC} center and the 1794 cm^{-1} absorption signal occur at similar temperatures with the annealing stage of the absorption signal lowered by ~ 25 K relative to the EH_{BC} . This is to be expected for annealing caused by migration to sinks as anticipated here. The infrared *in situ* study could only be done with samples containing a very high hydrogen concentration ($\sim 10^{18}\text{ cm}^{-3}$) with the consequence that the concentration of implantation induced vacancy-type defects is similar or even

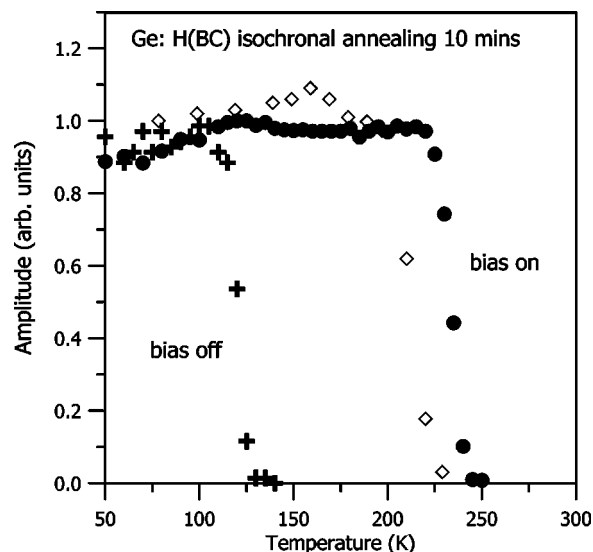


FIG. 5. Isochronal annealing steps for the donor signal. The zero-bias annealing (crosses) indicates a single-atomic-jump annealing with activation energy in the range $0.36\text{--}0.38$ eV. The reverse-bias step (filled circles) is compared to the annealing step of the 1794 cm^{-1} infrared absorption (open symbols) reproduced from Ref. 16. With a difference in prefactor by one order of magnitude due to different trap concentration in the two cases the (common) step correspond to an activation energy for migration in the range $0.48\text{--}0.52$ eV. See text for further details.

higher. The vacancy defects act as effective traps (sinks) for migrating hydrogen as indicated by the fact that characteristic vacancy-hydrogen centers are formed abundantly as a result of the annealing.¹⁶

The situation is different for the low-dose DLTS study. Here the induced vacancy concentration is many orders of magnitude lower and two other processes are responsible for the disappearance of the emission signal, namely the migration and trapping of hydrogen at the inadvertent impurities (oxygen, carbon, and silicon) in combination with drift towards the junction in the electric field of the diode space-charge layer. The observed shift in the annealing temperature indicates a change in the prefactor by little more than one order of magnitude and thereby (for similar trapping radii) a difference in the trap concentration by the same amount. This is fully consistent with the concentration of inadvertent impurities in the sample ($\sim 10^{17}\text{ cm}^{-3}$) as compared to the concentration of implantation-induced traps ($>10^{18}\text{ cm}^{-3}$) in the ir measurement. In addition the recorded capacitance signal will diminish as a result of redistribution of hydrogen in, and escape of hydrogen from, the monitored part of the space-charge layer. As a result the isochronal annealing will appear steeper than would be the case for pure homogenous trapping in accordance with the experimental data.

Taking the two sets of data together we estimate the migration barrier for H^+ to be $0.48\text{--}0.52$ eV and the prefactor of the EH_{BC} annealing to lie in the range $10^7\text{--}10^8\text{ s}^{-1}$. These figures are close to those obtained for H^+ migration in Czochralski-grown silicon³ in similar measurements, ~ 0.44 eV and $\sim 10^8\text{ s}^{-1}$. A parallel to the silicon case is found also for the zero-bias data (the cross symbols of Fig.

5). This isochronal annealing can be analyzed consistently, with activation energy and prefactor in the ranges of 0.36–0.38 eV and 10^{12} – 10^{13} s⁻¹. The corresponding figures for the silicon case were obtained as 0.293 eV and 3×10^{12} s⁻¹ and proven to characterize a single atomic jump process of H⁰ away from the bond-center site.¹⁰

C. Search for an acceptor level

The application of forward injection pulses to Au Schottky barriers on *n*-type Ge crystals may cause injection of holes and recharge of hole traps in the lower part of the Ge band gap as shown recently.^{24,25} We mentioned already that weak hole emission from shallow traps has been observed at low temperature prior to implantation, and further weak minority signals in the same rate window result from the implantation. However, due to their small magnitude, mutual overlap, and interference with the donor emission these signals could not be resolved. In contrast to this, a distinct hole-emission signal could be observed in the temperature range 165–190 K. This emission is identical to a signal previously assigned to the single acceptor state of the vacancy-oxygen complex in germanium.^{24,25} We take this observation as a strong indication that a thorough search in the temperature interval covering most of the lower part of the band gap should reveal a deep acceptor level of interstitial hydrogen if it exists.

The work of Ref. 16 identified a strong infrared-active center, which is stable up to about 150 K. This center was tentatively assigned as interstitial hydrogen in an antibonding configuration in the negative charge state. If it gives rise to an acceptor level in the lower part of the band gap this should be revealed as a substantial minority signal in the Laplace DLTS spectra. We failed to find such a signal when covering the band gap up to about $E_V+0.25$ eV corresponding to the temperature where the antibonding configuration becomes unstable.¹⁶ Because we expect the acceptor abundance to be significantly higher than the donor abundance ($\sim 30\%$ of the hydrogen implants as discussed in Sec. III A) we conclude that the acceptor level is either close to midgap or, more likely, very shallow or even buried in the valence band.

IV. DISCUSSION

A. Comparison with theory

The results and analysis carried out in the previous section strongly favor the bond-center assignment of the metastable donor center generated by the low-temperature hydrogen implantation. We summarize the experimental evidence leading to this assignment. (1) The center is abundantly formed accounting for $\sim 30\%$ of the implants and is the dominant electrical center found in the upper ~ 0.25 eV of the band gap. (2) The center is trigonal, consistent with the position of hydrogen on the $\langle 111 \rangle$ axis of the Ge crystal. (3) The reverse-bias annealing of the center matches the annealing of the infrared absorption assigned previously as bond-center hydrogen. (4) The zero-bias and reverse-bias anneal-

ing of the center parallels the annealing of bond-center hydrogen in Si.

The bond-center assignment and metastability is in full accordance with the theoretical expectations as reviewed in Ref. 3. The analogous behavior of hydrogen in Si and Ge was pointed out in early theoretical work.¹⁴ It is well established experimentally that the presence of isolated hydrogen always counteracts the prevailing doping of *n*- or *p*-type Si. This amphoteric behavior has now become widely recognized as a common property of interstitial hydrogen in a number of semiconductor materials. Van de Walle¹⁵ compared the amphoteric properties for a number of cases applying a band alignment model. The basic assumption is the constancy on an absolute energy scale of the point where formation energies of H_{BC}^+ and H_T^- are equal. The position of the energy gap on this scale relative to this H_{BC}^+/H_T^- transition level determines the Fermi-level ranges in the gap where an added hydrogen impurity will act as acceptor or donor, or stay neutral. When the defect is of negative-*U* type, then the neutral situation never occurs in equilibrium. In consequence hydrogen is always negatively charged when the transition level is close to the edge of the valence band and positively charged when it is close to the edge of the conduction band. When the H_{BC}^+/H_T^- transition occurs well inside the gap the addition of hydrogen will tend to move the Fermi level towards pinning at the transition level. For Ge the explicit calculations¹⁴ and the systematics¹⁵ predict the transition level to be at the bottom of the band gap with a consequence that hydrogen at or near the tetrahedral interstitial site should give rise to a shallow acceptor level or a valence-band resonance and thereby compensate the *n*-type conductivity and possibly enhance *p*-type conductivity in germanium. This is in contrast to the amphoteric behavior of interstitial hydrogen in Si. The failure of our search for minority-carrier emission as described in Sec. III C supports this theoretical prediction.

Another theoretical prediction that is relevant to consider in the present context is the trend²⁶ indicated by calculation for the C, Si, Ge host sequence that the energy difference $E(H_T^0) - E(H_{BC}^0)$ is positive for Si and negative for Ge. The lowering of $E(H_T^0)$ would appear to provide a qualitative explanation for the experimental result (see Sec. III A) that the likelihood of a direct formation of metastable H_{BC}^0 is reduced by about a factor of two for Ge as compared to Si. The entering of hydrogen into a bond-center configuration requires a substantial lattice relaxation. In the case of silicon the high probability of H_{BC}^0 formation has been ascribed to a channel where hydrogen approaches thermalization as H_T^0 and then in the final stages of this process surpasses an “effective” barrier for entering the BC site.^{4,5} For Ge such “quasi-thermal” channel may be less efficient. The combination of the theoretical prediction²⁵ with the experimental results that the activation energy for the thermal process $H_{BC}^0 \rightarrow H_T^0$ is significantly larger for Ge than for Si indicates a high thermal barrier for the reverse process also. Further, the rate of the competing electron capture to form H_T^- is expected to increase when this hydrogen state is resonant with the valence band as indicated by our analysis. For both Ge and Si we do observe a measurable increase in production yield

($\sim 25\%$ and 10% , respectively) when the implantation temperature is increased from 50 K to 80 K. Obviously, full thermal equilibrium is not established during implantation. However, guided by the properties of the thermal barriers, we may conjecture that the formation of H_{BC}^0 results from jumps of hydrogen across an effective quasithermal barrier in competition with electron capture to form H_T^- , and that this competition is less favorable for the H_{BC}^0 formation in Ge than in Si with the reduced yield as a consequence.

B. Comparison with other measurements

In Sec. III B, as a key point in our data interpretation, we have already compared the annealing properties of our data with those of Ref. 16. As briefly mentioned in Sec. III C this *in situ* work also revealed the presence of a strong infrared absorption signal ascribed to a negatively charged antibonding or displaced *T*-site configuration of interstitial hydrogen. It is tempting to assume, considering its strength, that this signal may originate from the possible acceptor resonance discussed above. We may further compare our observations with properties of the known centers $A(H,C)$ and $A(H,Si)$ in germanium. These centers were generated in ultrapure material by rapid quenching from high temperature¹⁸ and examined in detail¹⁹ by photothermal ionization spectroscopy. They have trigonal symmetry like the antibonding-type center of Ref. 16. This coincidence of symmetry together with the theoretical expectation¹⁴ that all three centers should have similar energy levels may be taken as further support

for the assumed origin of the infrared signal. We have already mentioned in the introduction that muon data indicates that the activation energy for electron emission from the BC configuration is ~ 0.23 eV. This result differs from our result ~ 0.11 eV significantly more than for the Si case where the corresponding figures are ~ 0.21 eV and ~ 0.175 eV, respectively. We have no explanation for this apparent discrepancy.

V. CONCLUSIONS

We have identified the donor level of a metastable trigonal center of isolated hydrogen in *n*-type Ge. The center is assigned to the bond-center hydrogen as a result of the analysis of its formation and annealing properties and symmetry. It is the analog of the well-established bond-center configuration of isolated hydrogen in Si. A search for the complementary interstitial-site acceptor level failed, indicating that this level is very shallow or resonant with the valence band. Our experimental results comply with theoretical expectations.

ACKNOWLEDGMENTS

This work has been supported by the Danish National Research Foundation through the Aarhus Center for Atomic Physics (ACAP), the U.K. Engineering and Physical Science Research Council, and the State Committee for Scientific Research Grant No. 4T11B02123 in Poland. We thank Dr V.V. Litvinov (Belarussian State University, Minsk) for providing us with Ge samples and Pia Bomholt, E. Łusakowska, D. Dobosz, and W. Choińska for sample preparations.

*Email address: dobacz@ifpan.edu.pl

¹See *Hydrogen in Semiconductors*, Vol. 34 of Semiconductors and Semimetals, edited by J. I. Pankove and N. M. Johnson (Academic Press, New York, 1991), and references therein.
²See *Hydrogen in Semiconductors II*, Vol. 61 of Semiconductors and Semimetals, edited by N. H. Nickel (Academic Press, New York, 1999), and references therein.
³S. K. Estreicher, *Mater. Sci. Eng.*, **R**, **14**, 314 (1995).
⁴K. Bonde Nielsen, B. Bech Nielsen, J. Hansen, E. Andersen, and J. U. Andersen, *Phys. Rev. B* **60**, 1716 (1999).
⁵C. Herring, N. M. Johnson, and C. G. Van de Walle, *Phys. Rev. B* **64**, 125209 (2001).
⁶K. Bonde Nielsen, L. Dobaczewski, S. Søgård, and B. Bech Nielsen, *Phys. Rev. B* **65**, 075205 (2002).
⁷C. G. Van de Walle, P. J. H. Denteneer, Y. Bar Yam, and S. T. Pantelides, *Phys. Rev. B* **39**, 10791 (1989).
⁸K. J. Chang and D. J. Chadi, *Phys. Rev. Lett.* **62**, 937 (1989).
⁹A. Van Wieringen and N. Warmoltz, *Physica (Amsterdam)* **22**, 849 (1956).
¹⁰B. Holm, K. Bonde Nielsen, and B. Bech Nielsen, *Phys. Rev. Lett.* **66**, 2360 (1991).
¹¹Yu. V. Gorelkinskii and N. N. Nevynnyi, *Physica B* **170**, 155 (1991).
¹²S. R. Kreitzman, B. Hitti, R. L. Lichti, T. L. Estle, and K. H. Chow, *Phys. Rev. B* **51**, 13117 (1995).
¹³B. Hitti, S. R. Kreitzman, T. L. Estle, E. Bates, M. R. Dawdy, T.

L. Head, and R. L. Lichti, *Phys. Rev. B* **59**, 4918 (1999).
¹⁴P. J. H. Denteneer, C. G. Van de Walle, and S. Pantelides, *Phys. Rev. Lett.* **62**, 1884 (1989).
¹⁵C. G. Van de Walle, *Phys. Status Solidi B* **235**, 89 (2003).
¹⁶M. Budde, B. Bech Nielsen, C. Parks Cheney, N. H. Tolk, and L. Feldman, *Phys. Rev. Lett.* **85**, 2965 (2000).
¹⁷R. L. Lichti, S. F. Cox, K. H. Chow, E. A. Davies, T. L. Estle, B. Hitti, E. Mytilineou, and C. Schwab, *Phys. Rev. B* **60**, 1734 (1999).
¹⁸E. E. Haller, B. Joós, and L. M. Falicov, *Phys. Rev. B* **21**, 4729 (1980).
¹⁹J. M. Kahn, R. E. McMurray, E. E. Haller, and L. M. Falicov, *Phys. Rev. B* **36**, 8001 (1987).
²⁰L. Dobaczewski, P. Kaczor, I. D. Hawkins, and A. R. Peaker, *J. Appl. Phys.* **76**, 194 (1994).
²¹K. Bonde Nielsen and E. Andersen, *J. Appl. Phys.* **79**, 9385 (1996).
²²L. C. Kimerling, *J. Appl. Phys.* **45**, 1839 (1974).
²³J. L. Hartke, *J. Appl. Phys.* **39**, 4871 (1968).
²⁴J. Fage Pedersen, A. Nylandsted Larsen, and A. Mesli, *Phys. Rev. B* **62**, 10116 (2000).
²⁵V. P. Markevich, I. D. Hawkins, A. R. Peaker, V. V. Litvinov, L. I. Murin, L. Dobaczewski, and J. L. Lindström, *Appl. Phys. Lett.* **81**, 1821 (2002).
²⁶S. K. Estreicher, M. A. Roberson, and D. M. Maric, *Phys. Rev. B* **50**, 17018 (1994).